



Accurate Description of Photoionization Dynamical Parameters

Moitra, Torsha; Ponzi, Aurora; Koch, Henrik; Coriani, Sonia; Decleva, Piero

Published in:
The Journal of Physical Chemistry Letters

Link to article, DOI:
[10.1021/acs.jpcllett.0c01337](https://doi.org/10.1021/acs.jpcllett.0c01337)

Publication date:
2020

Document Version
Peer reviewed version

[Link back to DTU Orbit](#)

Citation (APA):
Moitra, T., Ponzi, A., Koch, H., Coriani, S., & Decleva, P. (2020). Accurate Description of Photoionization Dynamical Parameters. *The Journal of Physical Chemistry Letters*, 11(13), 5330-5337. <https://doi.org/10.1021/acs.jpcllett.0c01337>

General rights

Copyright and moral rights for the publications made accessible in the public portal are retained by the authors and/or other copyright owners and it is a condition of accessing publications that users recognise and abide by the legal requirements associated with these rights.

- Users may download and print one copy of any publication from the public portal for the purpose of private study or research.
- You may not further distribute the material or use it for any profit-making activity or commercial gain
- You may freely distribute the URL identifying the publication in the public portal

If you believe that this document breaches copyright please contact us providing details, and we will remove access to the work immediately and investigate your claim.

Accurate Description of Photoionization Dynamical Parameters. Supporting Information

Torsha Moitra,[†] Aurora Ponzi,[‡] Henrik Koch,[¶] Sonia Coriani,^{*,†} and Piero
Decleva^{*,§}

[†]*DTU Chemistry, Technical University of Denmark, Kemitorvet Bldg 207, DK-2800 Kgs.
Lyngby, Denmark*

[‡]*Department of Physical Chemistry, Institut Ruđer Bošković, 10000 Zagreb, Croatia*

[¶]*Scuola Normale Superiore, Piazza dei Cavalieri 7, I-56126 Pisa, Italy*

[§]*Dipartimento di Scienze Chimiche e Farmaceutiche, Università degli Studi di Trieste,
I-34121 Trieste, Italy*

E-mail: soco@kemi.dtu.dk; decleva@units.it

Definitions

Our objective is to compute the photoelectron transition moments between an initial (label I) and a final (label F) state

$$D^{FI} = \langle \Psi_F | \hat{\mu} | \Psi_I \rangle \quad (1)$$

where $\hat{\mu}$ is the dipole moment operator.

Following the works of Arneberg et al.,¹ we write the final state (Ψ_F) for the photoionization process as an antisymmetrized product of the wavefunction of the photoelectron (the continuum electron), ϕ_ϵ , and a bound $(N - 1)$ -electron wavefunction Ψ^{N-1} :

$$\Psi_F \equiv \Psi_{F\epsilon} = \mathcal{A}(\Psi_F^{N-1} \phi_\epsilon) = a_\epsilon^\dagger \Psi_F^{N-1} \quad (2)$$

The (transition) dipole operator in second quantization is

$$\hat{\mu} = \sum_{pq} \mu_{pq} a_p^\dagger a_q \quad (3)$$

where $\mu_{pq} = \langle \phi_p | \vec{\mu} | \phi_q \rangle$. Then, starting from the reduction of the many particle transition moments and neglecting the conjugate Dyson, one can arrive at the following expression

$$D_x^{FI} = \sum_q \langle \phi_\epsilon | \mu_x | \phi_q \rangle \gamma_q \equiv \langle \phi_\epsilon | \mu_x | \phi^d \rangle, \quad \phi^d = \sum_q \gamma_q \phi_q \quad (4)$$

Derivation of Eq. (4)

The derivation of Eq. (4) follows Martin and Shirley² and Arneberg et al.¹ We consider an orthonormal molecular orbital (MO) basis $\{\phi_p\}$ (of the initial state) with associated creation a_p^\dagger and annihilation a_p operators. We can expand the photoelectron function ϕ_ϵ on this basis

$$\phi_\epsilon = \sum_p \langle \phi_p | \phi_\epsilon \rangle \phi_p \quad (5)$$

whereby the corresponding creation and annihilation operators become

$$a_\epsilon^\dagger = \sum_p \langle \phi_p | \phi_\epsilon \rangle a_p^\dagger; \quad a_\epsilon = \sum_p \langle \phi_\epsilon | \phi_p \rangle a_p \quad (6)$$

Moreover

$$[a_p, a_q^\dagger]_+ = \delta_{pq}; \quad [a_\epsilon, a_q^\dagger]_+ = \langle \phi_\epsilon | \phi_q \rangle \quad (7)$$

From Eqs. (3) and (6), we can then write the transition dipole moment as

$$D^{FI} = \langle a_\epsilon^\dagger \Psi_F^{N-1} | \hat{\mu} | \Psi_I^N \rangle = \langle \Psi_F^{N-1} | a_\epsilon \hat{\mu} | \Psi_I^N \rangle = \sum_{pq} \mu_{pq} \langle \Psi_F^{N-1} | a_\epsilon a_p^\dagger a_q | \Psi_I^N \rangle \quad (8)$$

Using Eqs. (6) and (7) we rewrite

$$a_\epsilon a_p^\dagger a_q = \langle \phi_\epsilon | \phi_p \rangle a_q - a_p^\dagger a_\epsilon a_q = \langle \phi_\epsilon | \phi_p \rangle a_q + a_p^\dagger a_q a_\epsilon; \quad (9)$$

$$\begin{aligned} a_\epsilon \hat{\mu} &= \sum_{pq} \mu_{pq} a_\epsilon a_p^\dagger a_q \\ &= \sum_{pq} \mu_{pq} \langle \phi_\epsilon | \phi_p \rangle a_q - \sum_{pq} \mu_{pq} a_p^\dagger a_\epsilon a_q \\ &= \sum_q \sum_p \langle \phi_\epsilon | \phi_p \rangle \langle \phi_p | \vec{\mu} | \phi_q \rangle a_q + \left(\sum_{pq} \mu_{pq} a_p^\dagger a_q \right) a_\epsilon \\ &= \sum_q \langle \phi_\epsilon | \left(\sum_p |\phi_p\rangle \langle \phi_p| \right) \vec{\mu} | \phi_q \rangle a_q + \hat{\mu} a_\epsilon \\ &= \sum_q \langle \phi_\epsilon | \vec{\mu} | \phi_q \rangle a_q + \hat{\mu} a_\epsilon \\ &= \sum_q \langle \phi_\epsilon | \mu | \phi_q \rangle a_q + \hat{\mu} \sum_q \langle \phi_\epsilon | \phi_q \rangle a_q \end{aligned} \quad (10)$$

and finally arrive at

$$\begin{aligned}
D^{FI} &= \sum_q \langle \phi_\epsilon | \mu | \phi_q \rangle \langle \Psi_F^{N-1} | a_q | \Psi_I^N \rangle + \sum_q \langle \phi_\epsilon | \phi_q \rangle \langle \Psi_F^{N-1} | \hat{\mu} a_q | \Psi_I^N \rangle \\
&= \sum_q \langle \phi_\epsilon | \mu | \phi_q \rangle \gamma_q^F + \sum_q \langle \phi_\epsilon | \phi_q \rangle \eta_q^F
\end{aligned} \tag{11}$$

where we have introduced the definitions of the following amplitudes (expansion coefficients)

$$\gamma_q^F = \langle \Psi_F^{N-1} | a_q | \Psi_I^N \rangle; \quad \eta_q^F = \langle \Psi_F^{N-1} | \hat{\mu} a_q | \Psi_I^N \rangle \tag{12}$$

The first term in Eq. (11) is called the *direct* term, and the second one the *conjugate* term. According to Eq. (11), the full transition moment is given by 1-particle matrix elements with the continuum, multiplied by the γ_q^F and η_q^F amplitudes, which are matrix elements of the initial and final bound states. This is sufficient to get the cross section for a single channel calculation, with a product structure of the final wavefunction.

Introducing a resolution of identity on a set of $(N - 1)$ -electron wavefunctions into the conjugate term, we obtain

$$\langle \Psi_F^{N-1} | \hat{\mu} a_q | \Psi_I^N \rangle = \sum_J \langle \Psi_F^{N-1} | \mu | \Psi_J^{N-1} \rangle \langle \Psi_J^{N-1} | a_q | \Psi_I^N \rangle \tag{13}$$

$$\eta_q^F = \sum_J D_{N-1}^{FJ} \gamma_q^J \tag{14}$$

where D_{N-1}^{FJ} indicates the transition dipole moment between two electronic states of the $(N - 1)$ -electron ionic (bound) system. At high energy, or simply when the photoelectron wavefunction is considered orthogonal to all bound orbitals included in the expansion of the initial state, the conjugate term is negligible, and only the direct term survives.

Finally, introducing in the direct term the definition of the *Dyson orbital*, ϕ^d :

$$\phi^d = \sum_q \phi_q \gamma_q^F \tag{15}$$

we arrive at the expression for the transition moment already given in Eq. (4)

$$D_x^{FI} = \sum_q \langle \phi_\varepsilon | \mu_x | \phi_q \rangle \gamma_q^F \equiv \langle \phi_\varepsilon | \mu_x | \phi^d \rangle$$

At the independent particle level (unrelaxed Hartree-Fock configurations), we have that $\gamma_q = 1$ for the primary ionic states, and $\gamma_q = 0$ otherwise, i.e.

$$|\Psi_F^{N-1}\rangle = a_q |\text{HF}\rangle \tag{16}$$

Thus, those are the only final states that are allowed, and their corresponding Dyson orbitals are simply the canonical occupied Hartree-Fock (HF) orbitals ϕ_p , with unit norm.

The square norm of the Dyson orbital

$$R_F \equiv \|\phi^d\|^2 = \sum_p |\gamma_p^F|^2 \tag{17}$$

is often called *spectral strength* or *pole strength* of the final bound state.

Correlation lowers the spectral strengths of the primary ionic states, and gives intensity to additional states (satellite or shake-up states) characterized by additional electronic excitations. The usual values for the outermost primary states (outer valence) are about 0.8–1.00. The effects become especially strong for the inner valence region (higher ionic states of the same symmetry) mainly because of the mixing with 2h-1p configurations relative to outer excitations, and the spectral strength can spread over many final states of low intensity. Another important effect is the mixing of different canonical MOs in the Dyson orbital, due to rotation of the occupied orbitals upon ionization.

Photoelectron transition strength in the EOM-CC formalism

In coupled cluster (CC) theory, a transition strength (matrix element) between two states I and F is written as

$$S_{xy}^{IF} = \frac{1}{2} \{ D_x^{IF} D_y^{FI} + (D_y^{IF} D_x^{FI})^* \} \quad (18)$$

where the left and right moments are,

$$D_x^{IF} = \langle \Psi_I | \mu_x | \Psi_F \rangle^{(L)}; \quad D_x^{FI} = \langle \Psi_F | \mu_x | \Psi_I \rangle^{(R)} \quad (19)$$

The labels (L) or (R) are used to highlight that, in EOM-CC, the above are not true scalar products, since they are not Hermitian, $D_x^{FI} \neq (D_x^{IF})^*$. We can then write

$$\begin{aligned} D_x^{IF} &= \langle (\phi_{fi}^d)^L | \mu_x | \phi_\epsilon \rangle; & \phi_{fi}^L &= \sum_p \gamma_p^L \phi_p \\ D_x^{FI} &= \langle \phi_\epsilon | \mu_x | (\phi_{fi}^d)^R \rangle & \phi_{fi}^R &= \sum_p \gamma_p^R \phi_p \end{aligned} \quad (20)$$

From now onwards, we will use ϕ_{fi}^R instead of $(\phi_{fi}^d)^R$ and similarly for the left one. The transition moments in Eq. (20) are now true scalar products (as computed in our program) between the continuum and the left and right Dyson orbitals. Using the above expressions, we then consider the photoelectron transition strength matrix

$$S_{xy}^{FI} \equiv \langle \Psi_F | \mu_x | \Psi_I \rangle \langle \Psi_I | \mu_y | \Psi_F \rangle \quad (21)$$

$$= \frac{1}{2} [(\langle \phi_\epsilon | \mu_x | \phi_{fi}^R \rangle \langle \phi_{fi}^L | \mu_y | \phi_\epsilon \rangle) + (\langle \phi_\epsilon | \mu_y | \phi_{fi}^R \rangle \langle \phi_{fi}^L | \mu_x | \phi_\epsilon \rangle)^*] \quad (22)$$

$$= \frac{1}{2} [\langle \phi_\epsilon | \mu_x | \phi_{fi}^R \rangle \langle \phi_\epsilon | \mu_y | \phi_{fi}^L \rangle^* + \langle \phi_\epsilon | \mu_x | \phi_{fi}^L \rangle \langle \phi_\epsilon | \mu_y | \phi_{fi}^R \rangle^*] \quad (23)$$

Thus, in practice, any expression (in the original code for variational wavefunction) that contains Hermitian products of two dipole matrix elements is transformed (in the non-variational

CC case) as

$$D_{\alpha}^{FI}(D_{\beta}^{FI})^* \rightarrow \frac{1}{2} \{ D_{R,\alpha}^{FI} D_{L,\beta}^{IF*} + D_{L,\alpha}^{IF} D_{R,\beta}^{FI*} \} \quad (24)$$

where α and β refer to different cartesian components x , y or z , which is the form employed in Eq (30).

Calculation of the photoionization observables using the LCAO B-spline approach

The differential cross section is given by,

$$\frac{d\sigma}{dk} = 4\pi^2 \alpha \omega |\langle \Psi_F | \vec{\varepsilon}' \cdot \vec{\mu} | \Psi_i \rangle|^2 \quad (25)$$

The terms in Eq. (25) have usual meaning as defined in the main article.

To obtain the differential cross section, we first compute the continuum orbitals in the angular momentum representation

$$H\phi_{\epsilon,lm} = E\phi_{\epsilon,lm} \quad (26)$$

with real (K-matrix) boundary conditions, as well as the transition dipole moments with left and right Dyson orbitals ϕ^L and ϕ^R .

Then, $\phi_{\epsilon,lm}$ and the corresponding dipole moments are transformed to incoming-wave boundary conditions, $\phi_{\epsilon lm}^{(-)}$, and finally to $\phi_{\vec{k}}^{(-)}$, where

$$\phi_{\vec{k}}^{(-)} = \frac{1}{\sqrt{m}} \sum_{lm} i^l e^{-i\sigma_l} Y_{lm}^*(\hat{k}) \phi_{\epsilon lm}^{(-)} \quad (27)$$

Omitting, for ease of notation, the superscript FI , the left and right photoelectron dipole matrix elements (in Eq. (20)) are obtained as

$$D_{\ell m, \gamma}^R = \langle \phi_{\ell m}^{(-)} | \mu_\gamma | \phi_{fi}^R \rangle \quad (28)$$

and similarly for $D_{\ell m, \gamma}^L$. Following standard manipulations as adopted by Chandra,³ one obtains, for randomly oriented molecules,

$$\frac{d\sigma}{dk} = \pi\alpha\omega(-1)^{m_r} \sum_L A_L(k) P_L(\cos\theta) \quad (29)$$

where m_r specifies the polarization of light [$m_r = 0, +1, -1$ for linearly polarized (LP), left circularly polarized (LCP) and right circularly polarized (RCP) light, respectively]; θ is the angle between the momentum of the electron and either the polarization vector (for LP) or the direction of propagation (for CP) of the light beam. The coefficients $A_L(k)$ are given by

$$\begin{aligned} A_L(k) = (2L+1) & \begin{pmatrix} 1 & 1 & L \\ m_r & -m_r & 0 \end{pmatrix} \sum_{\substack{lm\gamma \\ l'm'\gamma'}} (-1)^{m+\gamma} \sqrt{(2l+1)(2l'+1)} \\ & \times \begin{pmatrix} l & l' & L \\ 0 & 0 & 0 \end{pmatrix} \begin{pmatrix} l & l' & L \\ -m & m' & (m-m') \end{pmatrix} \begin{pmatrix} 1 & 1 & L \\ \gamma' & -\gamma & (\gamma-\gamma') \end{pmatrix} \\ & \times \frac{1}{2} (D_{\ell m, \gamma}^R D_{\ell' m', \gamma'}^{L*} + D_{\ell m, \gamma}^L D_{\ell' m', \gamma'}^{R*}). \quad (30) \end{aligned}$$

Establishing the correspondences

$$\frac{\sigma}{4\pi} = \pi\alpha\omega(-1)^{m_r} A_0 \quad (31)$$

$$D = \frac{A_1(m_r = 1)}{A_0}; \quad \beta = \frac{A_2(m_r = 0)}{A_0} \quad (32)$$

we finally obtain the usual expression for the differential cross section ($m_r = \pm 1$),

$$\frac{d\sigma}{dk} = \frac{\sigma}{4\pi} \left[1 + m_r D \cos \theta - \frac{1}{2} \beta P_2(\cos \theta) \right] \quad (33)$$

or simply, for linear polarization ($m_r = 0$),

$$\frac{d\sigma}{dk} = \frac{\sigma}{4\pi} [1 + \beta P_2(\cos \theta)] \quad (34)$$

Parameters used in the LCAO B-spline code and in the ezDyson code

Table S1: Parameters used in the LCAO B-spline code. L_{\max} and l_{\max} are the maximum angular momentum employed in the one center expansion at origin and on each atom (off-center), respectively. R_{\max} and r_{\max} are the maximum radial grid length from origin and off-center atoms, respectively.

Molecule	# grid points	L_{\max}	R_{\max} (a.u.)	LCAO descriptor	
				r_{\max} (a.u.)	l_{\max}
Ar	125	2	25	-	-
CO	125	20	25	0.4(C,O)	2
CS	125	20	25	0.4(C,S)	2
H ₂ O	125	10	25	1.0(H)	2
CH ₂ O	100	12	25	0.2 (C,O,H)	2
C ₄ H ₄ O (planar)	100	15	25	1.0 (C,O,H)	2
C ₄ H ₄ O (bent)	100	15	25	1.0 (C,O,H)	2
(S)-C ₃ H ₆ O	50	12	25	0.6(O), 1.0(C,H)	2

Table S2: Parameters for calculations of cross-sections and asymmetry parameter using ezDyson⁴ code. L_{\max} is the maximum angular momentum number for which spherical waves are generated and the dipole matrix elements are calculated. E_k^{\min} and E_k^{\max} are the minimum and maximum value, respectively, of the kinetic energy for which the cross-section and asymmetry parameter are computed. $\langle R^2 \rangle$ is the average square radial distance, used for analyzing the size and shape of the left Dyson orbital.

Molecule	L_{\max}	# grid points	E_k^{\min} (eV)	E_k^{\max} (eV)	$\langle R^2 \rangle$ (Å)
Ar	2	101	0.1	100.1	0.608698
CO	5	101	0.1	100.1	1.052489
CS	5	101	0.1	100.1	1.697160
H ₂ O	5	50	0.5	50.5	0.763224
CH ₂ O	5	101	0.1	100.1	1.121095

Ionization energies (IE) and Dyson norms

Table S3: IE (in eV) and EOM-CCSD Dyson square norms of the ground state using aug-cc-pVTZ basis set. Experimental results are taken from Ref. 5 and 6. Mulliken’s symmetry convention is assumed.

System	Irrep	KT IE (eV)	EOM-CCSD IE (eV)	Dyson sq. norm ($ \phi^L \cdot \phi^R ^2$)	Exp. IE (eV)
Ar	3s	34.83	29.91	0.859	29.2
	3p	16.05	15.66	0.965	15.8
CO	5 σ	15.10	14.20	0.952	14.0
	4 σ	21.91	19.82	0.934	19.7
	1 π	17.41	17.10	0.949	16.9
CS	7 σ	12.82	11.52	0.931	11.3
	2 π	12.60	13.06	0.953	12.8
H ₂ O	3a ₁	15.92	14.83	0.957	14.7
	1b ₂	19.51	19.00	0.962	18.5
	1b ₁	13.88	12.62	0.956	12.6
CH ₂ O	5a ₁	17.77	16.15	0.944	16.0
	2b ₂	12.05	10.86	0.951	10.8
	1b ₁	14.64	14.66	0.944	14.5
C ₄ H ₄ O (planar)	1a ₂	8.68	9.04	0.950	8.8
	2b ₁	10.80	10.40	0.946	10.4
(S)- methyl- oxirane	16a	11.78	10.37	0.944	10.4
	15a	12.17	11.21	0.951	11.3
	14a	14.01	13.23	0.952	13.0
	13a	14.37	13.44	0.952	13.6
	12a	15.26	14.40	0.953	14.5
	11a	15.97	15.12	0.952	15.1

Partial cross-sections and asymmetry parameters

Argon

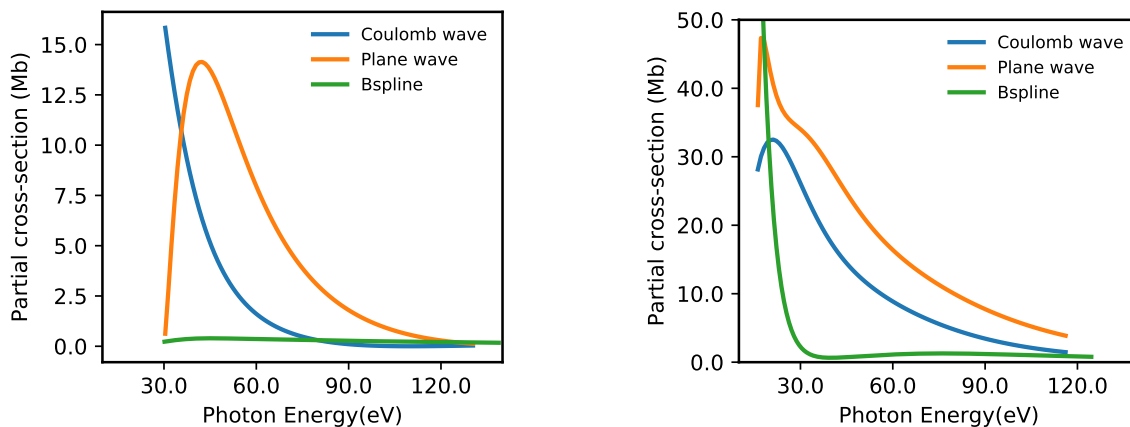


Figure S1: Partial cross-section of Ar relative to 3s (left) and 3p (right) states calculated with plane wave, coulomb wave and DFT-B-spline functions to represent the outgoing electron coupled with EOM-CCSD/aug-cc-pVTZ Dyson orbitals.

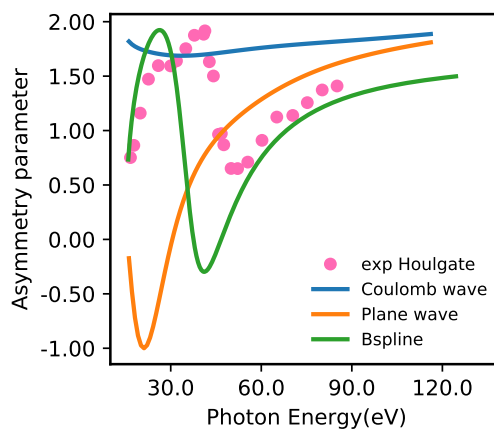


Figure S2: Comparative study of asymmetry parameter of Ar relative to ionization from 3p orbital. EOM-CCSD Dyson orbitals are used throughout. Experimental result taken from Ref. 7.

Carbon sulphide, CS

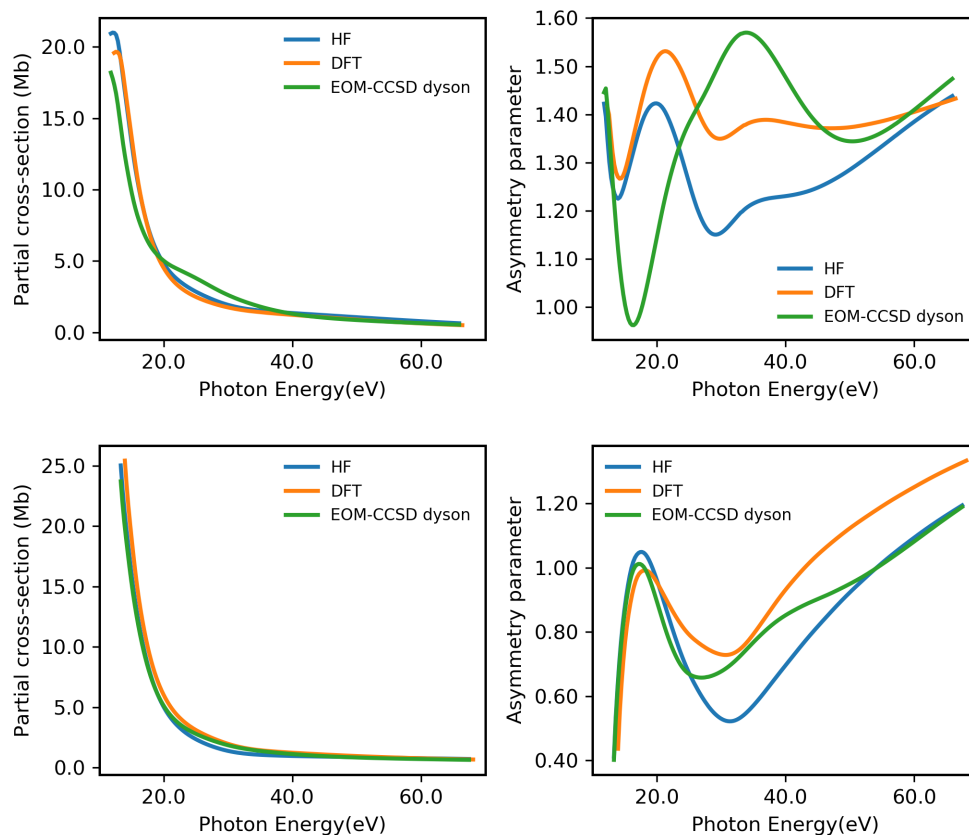


Figure S3: Partial cross-section and asymmetry parameters of CS relative to 7σ (top) and 2π (bottom) states calculated with HF, DFT and EOM-CCSD methods. Multicenter B-spline functions are used to describe the outgoing electron.

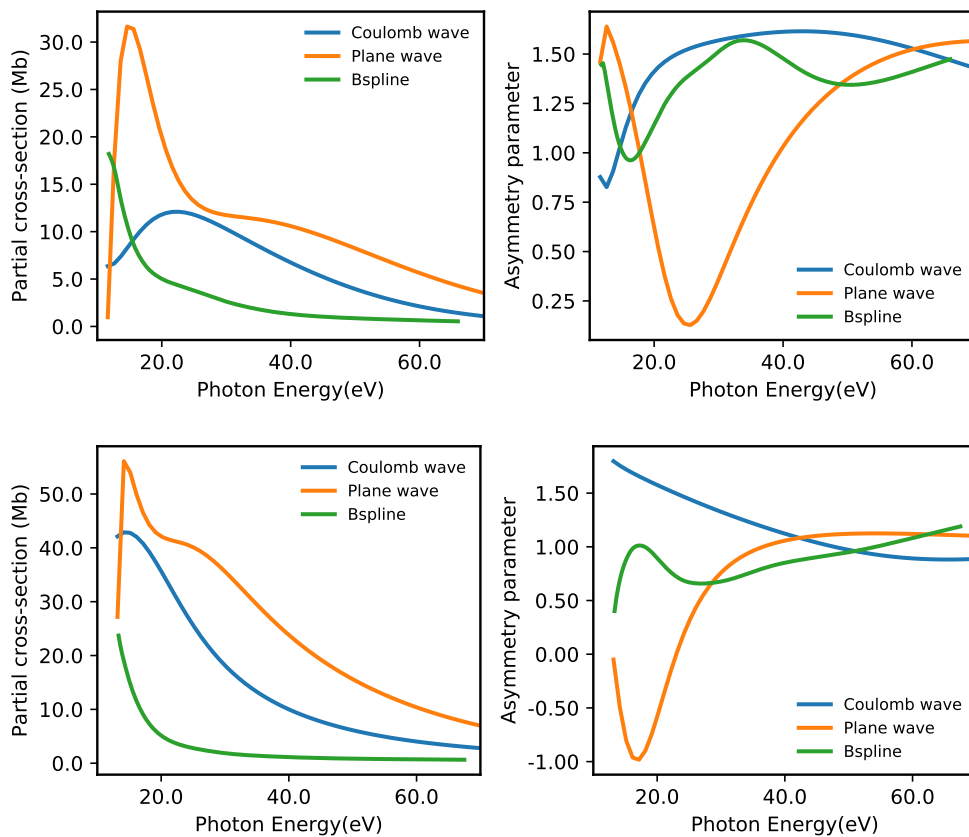


Figure S4: Partial cross-section and asymmetry parameters of CS relative to 7σ (top) and 2π (bottom) states calculated with plane wave, coulomb wave and B-spline functions to represent the outgoing electron coupled with EOM-CCSD/aug-cc-pVTZ Dyson orbitals.

Formaldehyde

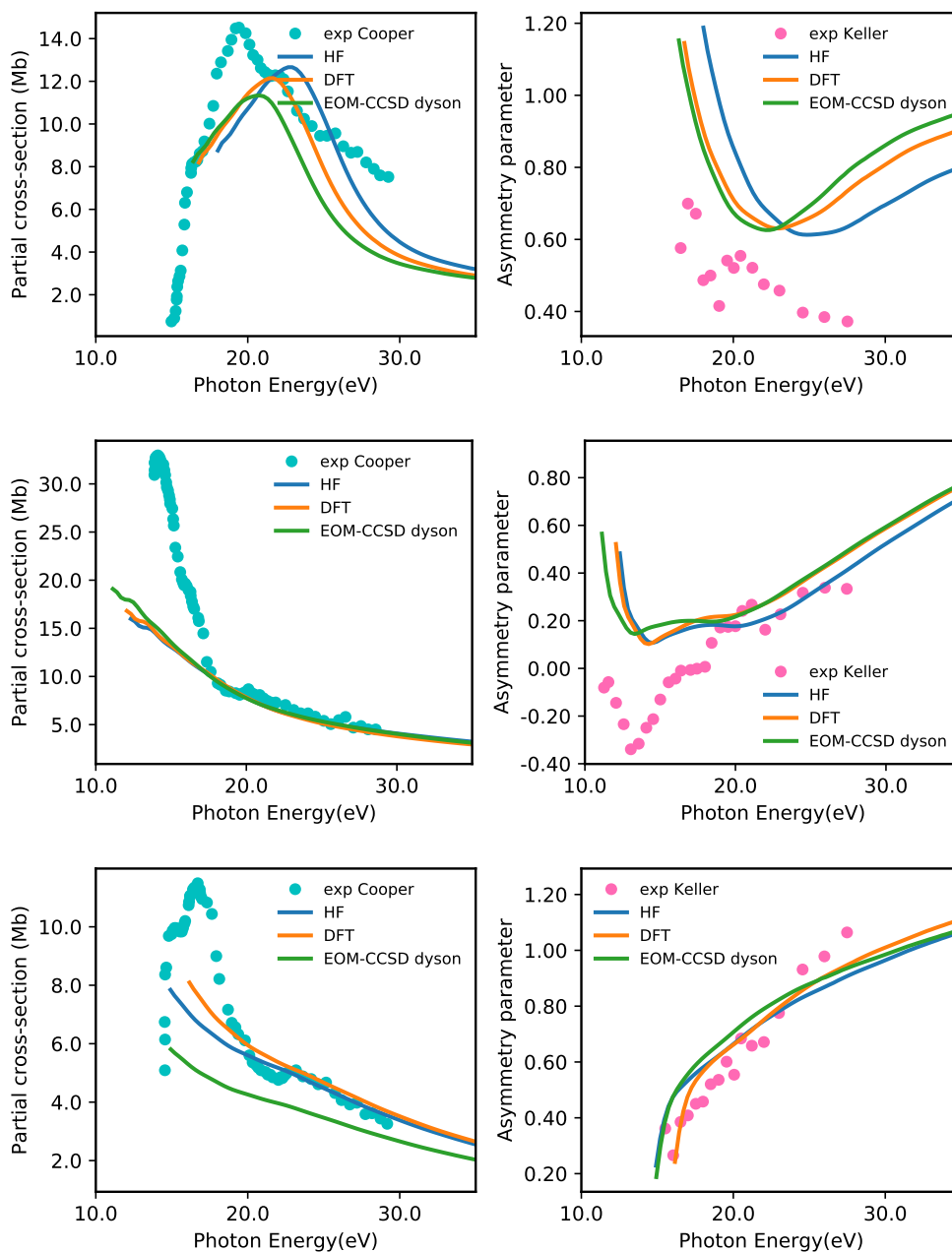


Figure S5: Partial cross-section and asymmetry parameters of CH₂O relative to 5a₁ (top) and 2b₂ (middle) and 1b₁ (bottom) states calculated with HF, DFT and EOM-CCSD methods. Multicenter B-spline functions are used to describe the outgoing electron. Experimental results are taken from Ref. 8 and 9.

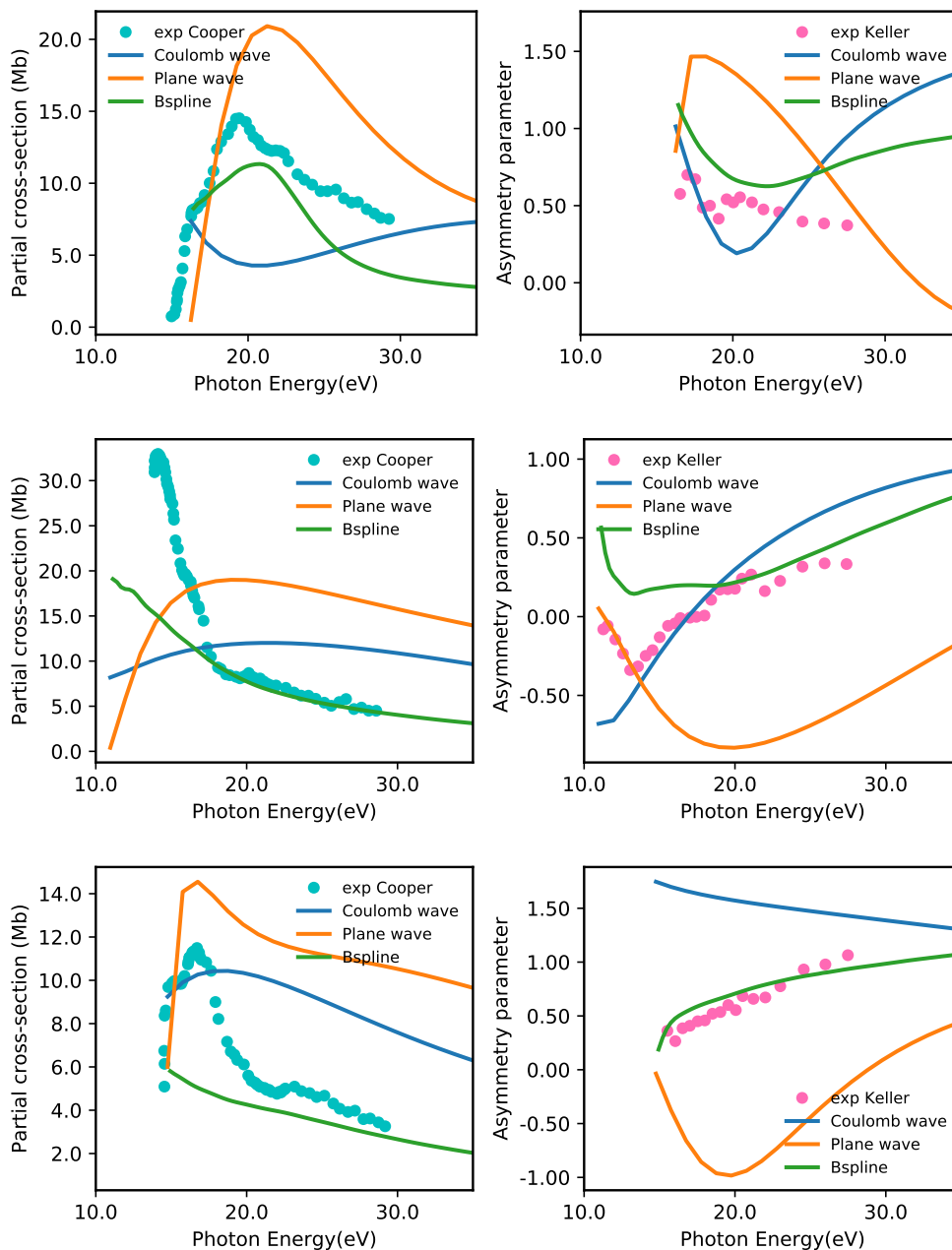


Figure S6: Partial cross-section and asymmetry parameters of CH₂O relative to 5a₁ (top) and 2b₂ (middle) and 1b₁ (bottom) states calculated with plane wave, coulomb wave and B-spline functions to represent the outgoing electron coupled with EOM-CCSD/aug-cc-pVTZ Dyson orbitals. Experimental results are taken from Ref. 8 and 9.

Excitation and ionization energies of furan

Table S4: Excitation energies of furan in eV. Experimental results are from Ref. 6. CASSCF, NEVPT2, TDDFT and ADC(2) results are from Ref. 10.

Geometry	State	EOM-CCSD	CAS-[6,9]	NEVPT2	TDDFT	ADC(2)	Exp.
Planar	1A_2 (S_1)	6.15	5.71	5.98	5.51	5.91	6.04
	1B_2 (S_2)	6.47	6.91	6.63	5.98	6.44	6.49
Bent	1A	2.11	-	-	-	-	-
	1A	3.85	-	-	-	-	-

Table S5: Ionization energy from the excited state of furan in eV. CASSCF results are from Ref. 10

Geometry	Excited state	Ionized state of cation	EOM-IP-CCSD	CAS-[6,9]
Planar	1A_2 (S_1)	2A_2	2.89	2.43
	1B_2 (S_2)	2A_2	2.57	1.23
Bent	1A (S_1)	2A	5.23	4.22
	1A (S_2)	2A	3.48	2.96

Excited state cross-section and asymmetry parameter of furan at bent geometry

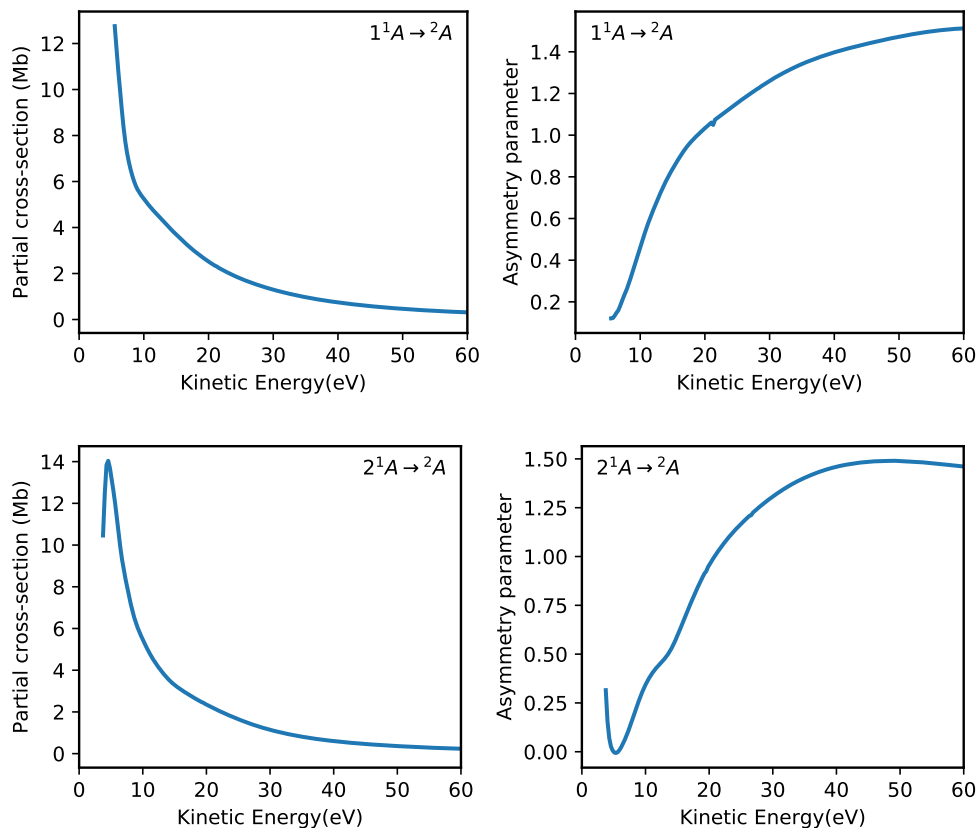


Figure S7: Computed photoionization partial cross section (left) and photoelectron asymmetry parameter (right) for transition from S_1 (top) and S_2 (bottom) states of furan at a puckered geometry.

Cartesian coordinates of all molecules

CO (Angs)

O	0.00000000	0.00000000	0.48356580
C	0.00000000	0.00000000	-0.64475440

H₂O (Angs)

O	-0.00000000	-0.00000000	0.11730000
H	-0.75720000	-0.00000000	-0.46920000
H	0.75720000	0.00000000	-0.46920000

CS (Angs)

S	0.00000000	0.00000000	0.41860909
C	0.00000000	0.00000000	-1.11629091

CH₂O (Angs)

O	0.00000000	0.00000000	0.67595000
C	0.00000000	0.00000000	-0.52905000
H	0.94290000	0.00000000	-1.11665000
H	-0.94290000	-0.00000000	-1.11665000

C₄H₄O (Angs)-Planar

O	0.00000000	0.00000000	1.15570089
C	-0.71808000	0.00000000	-0.96094011
C	0.71808000	0.00000000	-0.96094011
C	-1.09300200	0.00000000	0.35220389
C	1.09300200	0.00000000	0.35220389

H	2.05718500	0.00000000	0.85420589
H	-2.05718500	0.00000000	0.85420589
H	1.37995400	0.00000000	-1.82459211
H	-1.37995400	0.00000000	-1.82459211

C₄H₄O (Angs)- Bent

O	1.09645392	-0.24983976	-0.34616477
C	0.64775401	0.90476604	0.14769665
C	-0.87836149	0.84558708	-0.05929252
C	-1.07423176	-0.47773249	-0.13303448
C	0.19506068	-1.05871585	0.15814657
H	1.19377197	1.61166861	0.79100107
H	-1.51941099	1.72028223	0.01907603
H	-1.97177413	-1.14269353	0.02025521
H	0.18445315	-1.47396792	1.25788853

C₃H₆O (au)

C	-0.28956361	0.08176958	0.92701577
C	1.93885200	-1.15600766	-0.10800484
C	-2.79852375	-0.19094696	-0.27656907
O	1.53613696	1.47730615	-0.46998636
H	1.71860882	-2.32670888	-1.80795335
H	3.52273536	-1.64526642	1.13875511
H	-0.27744501	0.50560530	2.96417187
H	-2.56905279	-0.59002862	-2.30639911
H	-3.89960425	1.56511541	-0.07933409
H	-3.88892566	-1.73605572	0.59599929

References

- (1) Arneberg, R.; Müller, J.; Manne, R. Configuration interaction calculations of satellite structure in photoelectron spectra of H₂O. *Chem. Phys.* **1982**, *64*, 249 – 258.
- (2) Martin, R. L.; Shirley, D. A. Theory of core-level photoemission correlation state spectra. *J. Chem. Phys.* **1976**, *64*, 3685–3689.
- (3) Chandra, N. Photoelectron spectroscopic studies of polyatomic molecules. I. Theory. *J. Phys. B: At. Mol. Phys.* **1987**, *20*, 3405–3415.
- (4) Gozem, S.; Krylov, A. I. *ezDyson*. Version 4.0 (accessed February 2020).
- (5) Jonathan, N.; Morris, A.; Okuda, M.; Ross, K. J.; Smith, D. J. Photoelectron spectroscopy of transient species. The CS molecule. *Faraday Discuss. Chem. Soc.* **1972**, *54*, 48–55.
- (6) Kimura, K. *Handbook of HeI photoelectron spectra of fundamental organic molecules: ionization energies, ab initio assignments, and valence electronic structure for 200 molecules*; Japan Scientific Societies Press, 1981; Includes indexes.
- (7) Houlgate, R.; West, J.; Codling, K.; Marr, G. The angular distribution of the 3p electrons and the partial cross section of the 3s electrons of argon from threshold to 70 eV. *J Electron Spectros Relat Phenomena* **1976**, *9*, 205 – 209.
- (8) Cooper, G.; Anderson, J. E.; Brion, C. E. Absolute photoabsorption and photoionization of formaldehyde in the VUV and soft X-ray regions (3–200 eV). *Chem. Phys.* **1996**, *209*, 61–77.
- (9) Keller, P.; Taylor, J.; Grimm, F.; Carlson, T. A. Angle-resolved photoelectron spectroscopy of formaldehyde and methanol. *Chem. Phys.* **1984**, *90*, 147 – 153.

- (10) Ponzi, A.; Sapunar, M.; Angeli, C.; Cimiraglia, R.; Došlić, N.; Decleva, P. Photoionization of furan from the ground and excited electronic states. *J. Chem. Phys.* **2016**, *144*, 084307.